Intra-cochlear differences in the spread of excitation between biphasic and triphasic pulse stimulation in cochlear implants: a modeling and experimental study

Herrmann, D.P.; Kalkman, R.K.; Frijns, J.H.M.; Bahmer, A.

Hearing Research 432 (2023) 108752

Contents lists available at ScienceDirect

Hearing Research

journal homepage: www.elsevier.com/locate/heares

Research Paper

Intra-cochlear differences in the spread of excitation between biphasic and triphasic pulse stimulation in cochlear implants: A modeling and experimental study

David P. Herrmann[a,1,*], Randy K. Kalkman[b,1], Johan H.M. Frijns[b,c], Andreas Bahmer[a,2]

[a] Department of Otorhinolaryngology, Plastic, Aesthetic and Reconstructive Head and Neck Surgery and the Comprehensive Hearing Center, University Hospital Würzburg, Josef-Schneider-Str. 11, Würzburg 97080, Germany
[b] Department of Otorhinolaryngology and Head & Neck Surgery, Leiden University Medical Centre, PO Box 9600, RC Leiden 2300, the Netherlands
[c] Leiden Institute for Brain and Cognition, PO Box 9600, RC Leiden 2300, the Netherlands

ARTICLE INFO

Article history:
Received 6 February 2022
Revised 21 March 2023
Accepted 27 March 2023
Available online 28 March 2023

Keywords:
Cochlear implant
Computational modeling
Experimental measurements
Electrical stimulation
Spread of excitation
Triphasic pulse

ABSTRACT

Triphasic pulse stimulation can prevent unpleasant facial nerve stimulation in cochlear implant users. Using electromyographic measurements on facial nerve effector muscles, previous studies have shown that biphasic and triphasic pulse stimulations produce different input-output functions. However, little is known about the intracochlear effects of triphasic stimulation and how these may contribute to the amelioration of facial nerve stimulation.

The present study used a computational model of implanted human cochleae to investigate the effect of pulse shape on the intracochlear spread of excitation. Biphasic and triphasic pulse stimulations were simulated from three different cochlear implant electrode contact positions. To validate the model results, experimental spread of excitation measurements were conducted with biphasic and triphasic pulse stimulation from three different electrode contact positions in 13 cochlear implant users.

The model results depict differences between biphasic and triphasic pulse stimulations depending on the position of the stimulating electrode contact. While biphasic and triphasic pulse stimulations from a medial or basal electrode contact caused similar extents of neural excitation, differences between the pulse shapes were observed when the stimulating contact was located in the cochlear apex. In contrast, the experimental results showed no difference between the biphasic and triphasic initiated spread of excitation for any of the tested contact positions. The model was also used to study responses of neurons without peripheral processes to mimic the effect of neural degeneration. For all three contact positions, simulated degeneration shifted the neural responses towards the apex. Biphasic pulse stimulation showed a stronger response with neural degeneration compared to without degeneration, while triphasic pulse stimulation showed no difference.

As previous measurements have demonstrated an ameliorative effect of triphasic pulse stimulation on facial nerve stimulation from medial electrode contact positions, the results imply that a complementary effect located at the facial nerve level must be responsible for reducing facial nerve stimulation.

1. Introduction

Cochlear implants (CIs) can restore hearing in patients with severe to profound sensorineural hearing loss by applying electrical current to auditory nerve fibers (ANFs) via intracochlear electrodes. Despite the CI's great success for many patients, negative side effects can occur in rare cases, such as the unintentional co-stimulation of the facial nerve, which runs in the vicinity of the cochlea (Bigelow et al., 1998; Kempf et al., 1999; Muckle and Levine, 1994; Niparko et al., 1991). Facial nerve stimulation (FNS) is predominantly observed in CI users who require high stimulation levels, for example in cases of otosclerosis (Bigelow et al., 1998;

Abbreviations: ANF, Auditory nerve fibers; ANOVA, analysis of variance; ART, aligned-rank transform; BM, basilar membrane; BP, biphasic pulse; CI, cochlear implant; CU, current units; ECAP, evoked compound action potential; ED, excitation density; FNS, facial nerve stimulation; MCL, most comfortable loudness; PECAP, panoramic evoked compound action potential, RIB2, research interface box 2; RMS, root mean square; SNR, signal to noise ratio; SOE, spread of excitation; ThP, threshold profile; THR, threshold; TP, triphasic pulse.

* Corresponding author.
E-mail address: herrmann_d@ukw.de (D.P. Herrmann).
[1] These authors equally contributed equally to this work.
[2] RheinMain University of Applied Sciences, Campus Rüsselsheim, Am Brückweg 26, 65428 Rüsselsheim, Germany

https://doi.org/10.1016/j.heares.2023.108752
0378-5955/

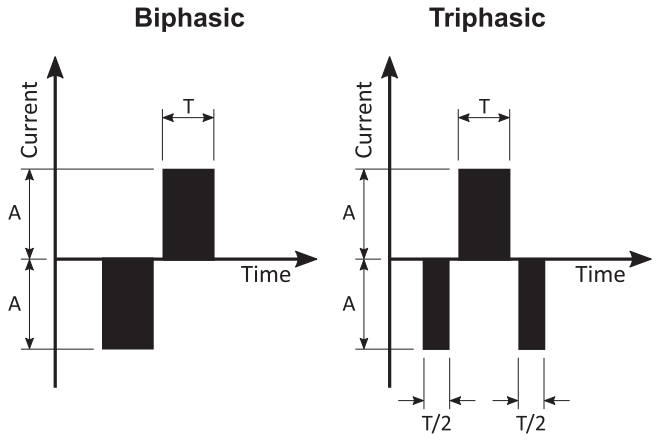

Fig. 1. Cathodic first phase biphasic pulse (BP) and triphasic pulse (TP). The stimulation amplitudes of the pulses are marked by A, and the phase durations are marked by T. For the triphasic pulse, the phase duration of the first and third phases is half the duration of the second phase.

Kempf et al., 1999; Muckle and Levine, 1994; Pires et al., 2018; Polak et al., 2006; Rayner et al., 2003; Rotteveel et al., 2004; Seyyedi et al., 2013), trauma of the temporal bone (Pires et al., 2018), labyrinthitis ossificans (Nassiri et al., 2018), and malformations of the cochlea (Seyyedi et al., 2013). As a consequence, stimulation amplitudes below the level of maximum comfortable loudness (MCL) can cause symptoms ranging from simple awareness to painful muscle spasms around the eyes and mouth (Berrettini et al., 2011). FNS is often triggered by medial electrode contacts located in the superior segment of the cochlear basal turn (Bigelow et al., 1998; Kelsall et al., 1997). It is assumed that this is caused by the close proximity of the lateral wall of the cochlea to the labyrinthine segment of the facial nerve at this position (Berrettini et al., 2011).

In the literature, incidences of FNS after CI implantation vary between 0.9 and 14.6% (Berrettini et al., 2011) and can be as high as 75% in patients with otosclerosis (Bigelow et al., 1998; Muckle and Levine, 1994). Furthermore, the occurrence of FNS correlates with certain factors such as anatomical characteristics (Schart-Moren et al., 2017) and the shape of the CI electrode array itself (Frijns et al., 2009a). In a computational model of implanted human cochleae and the facial nerve, otosclerotic changes coincided with an increase in the MCL and auditory threshold levels (THRs) of ANFs, whereas FNS thresholds changed only to a lesser extent (Frijns et al., 2009a). These elevated stimulation levels may be due to current leaking from the cochlea when the electrical conductivity of the temporal bone surrounding the cochlea increases (Frijns et al., 2009a). Previously investigated approaches for reducing FNS were prolonging the stimulation pulse duration or deactivating affected electrode channels. However, these measures can detrimentally affect the hearing performance of CI users (Crew et al., 2012; Dorman et al., 1997; Shannon et al., 1995). In severe cases of FNS, patients have undergone reimplantation or could not benefit from the CI at all (Battmer et al., 2006; Gärtner et al., 2022; Polak et al., 2006). In the standard stimulation mode, most current CI systems use biphasic pulses (BPs) for stimulation, namely pulses consisting of two consecutive phases of opposing polarity (see Fig. 1 left side), to prevent the emergence of neurotoxic products due to remaining electrical charge (Brummer and Turner, 1977; Lilly et al., 1955; Rowland et al., 1960). To balance the charge of each pulse, both phases are equal in the duration and absolute value of their amplitude. Recent studies have demonstrated that using a charge-balanced triphasic pulse (TP) with a cathodic first phase can significantly reduce FNS (Alhabib et al., 2020; Bahmer et al., 2017; Bahmer and Baumann, 2016; Braun et al., 2019). This alternative shape consists of two phases of the same polarity separated by one phase of opposing polarity. While the absolute amplitudes of all three phases are equal, TPs balance the charge by reducing the duration of the first and third phases to half that of the second phase (see Fig. 1 right side). As neurons are sensitive to short-term temporal charge differences, the differences in the temporal distribution of anodic and cathodic charges between the BPs and TPs produce different neural responses (Bahmer and Baumann, 2013; Herrmann et al., 2021).

The mechanism of the FNS-reducing effect of TPs remains unclear. Bahmer et al. (2017) recorded the extent of FNS in intraoperative electromyographic measurements for BPs and TPs with increasing stimulation levels. They suggested that the FNS-reducing effect of TPs could be attributed to the shallower slope of their input-output function compared to BP stimulation. The underlying process and its location, however, could not be determined and were suggested for further investigation. A possible explanation could be a difference in the response of cochlear and facial nerve fibers to BP and TP stimulations or that TP stimulation may generate a different spread of excitation (SOE) than BP stimulation in the cochlea. The present study evaluated this hypothesis using two approaches.

The first approach applied a computational model and calculated responses to BP and TP stimulations. The SOE was estimated from the simulated neural responses. The model was a detailed computational model of an implanted human cochlea from the Leiden University Medical center (Briaire and Frijns, 2006, 2005, 2000a, 2000b; Frijns et al., 2011, 2009b, 2009a, 2001, 2000; Kalkman et al., 2022, 2015, 2014; Snel-Bongers et al., 2013). It combined a volume conduction model based on the boundary element method and a deterministic active nerve fiber model (Frijns et al., 1995). The volume conduction model in the present study consisted of a realistic representation of the human cochlea implanted with a CI electrode array that satisfied the technical specifications of the Standard electrode type from the manufacturer MED-EL (Innsbruck, Austria). It contained five individual three-dimensional human cochlear geometries based on individual histological or radiological data. Each geometry described the boundaries between different intracochlear media, which were considered purely resistive with isotropic electrical conductivity values. The purpose of the model was to simulate the distribution of electrical potentials as a result of monopolar stimulation via the electrode contacts, particularly along the nerve fiber trajectories. Electrical potentials were passed to the deterministic nerve model, which simulated the response of the neurons. All the nerve fibers in the model were designed as active electrical double cables with an imperfectly insulating myelin sheath and a peri–axonal layer between the myelin and axon, as described by Dekker et al. (2014) and Kalkman et al. (2022). For each of the five cochlear geometries, a set of 3200 auditory neurons grouped in 80 bundles were implemented with the cell bodies and neural trajectories distributed in a pseudo-randomized fashion (Kalkman et al., 2015). Comparable to previous studies, an additional degenerated condition was generated for each cochlear geometry by removing all peripheral processes from the nerve fibers described above (Briaire and Frijns, 2006; Kalkman et al., 2022, 2015, 2014; Snel-Bongers et al., 2013).

The second approach to investigate possible differences between biphasic- and triphasic-stimulated SOEs consisted of electrophysiological measurements of electrically evoked compound action potentials (ECAPs). Cohen et al. (2003) first introduced a method to estimate the SOE by means of ECAP recordings. The method requires a forward-masking paradigm (Abbas et al., 1999; Miller et al., 2000) with the probe pulse fixed to one electrode contact while a masker pulse is varied across the electrode ar-

ray. The resulting ECAP amplitude is thought to represent the overlap between the neural excitation of the probe and masker pulses. Hence, the largest ECAP response should be measured when masker and probe are emitted from the same electrode contact. The ECAP amplitudes will decrease progressively as the distance between the masker and probe increases (Hughes, 2008). Cohen's SOE method was first used to compare biphasic- and triphasic-stimulated SOEs by Bakhos et al. (2013). Their results suggested that TPs with an anodic first phase could reduce the SOE. However, the TP shape they used and its polarity was not identical to that used in MED-EL's CI systems for reducing FNS. Moreover, Bakhos et al. (2013) matched the neural excitation stimulated by BP stimulation and TP stimulation using a psychophysical loudness balancing. In contrast, this study evaluated the intracochlear effect of BP and TP stimulation with pulse shapes and polarities used in the clinical setting. Instead of psychophysical procedures, which are often time consuming and can be influenced by learning, adaption and/or accommodation effects (Miller et al., 2008), the neural excitation by BPs and TPs in the measurements of this study was balanced using biphasic- and triphasic-stimulated ECAP amplitudes. It was decided to use the ECAP measurement as it provides an objective measure of intracochlear excitation. It is recorded proximal and consequently bypasses the higher auditory system. ECAPs were therefore considered to have the advantage over psychophysical procedures in producing results with lower variance.

2. Materials and methods

2.1. Stimuli

The model simulations and experimental measurements were conducted using the same stimuli (BPs and TPs) delivered in monopolar stimulation mode. Fig. 1 depicts the shape of the BPs and TPs used. BPs consist of two phases of opposing polarity with the same duration T, while TPs consist of three alternating phases where the second phase has a duration T and the first and third phases have a duration of T/2. The stimulating pulse phases are interrupted by an inter-phase gap. This study only used pulses with an initial cathodic phase. For all the pulses, T was set to 30 μs and the inter-phase gap was set to 2.1 μs. The stimulation levels were specified in current units (CU), with 1 CU corresponding to approximately 1 μA.

2.2. Computational model

The volume conduction model was based on the boundary element method and was used to calculate electrical potential fields in a three-dimensional geometrical representation of a human cochlea implanted with an electrode array under quasi-static conditions. The model contained the same five individual cochlear geometries, labeled CM1 through CM5, that were used previously by Kalkman et al. (2022). CM1 and CM2 were constructed from histological cross sections, while CM3, CM4, and CM5 were derived from microcomputed tomography reconstructions. Each geometry was implanted with a MED-EL Standard electrode array, with the exception of CM2, which was too small to contain the full active length of the Standard array and was instead implanted with a MED-EL Medium array. In addition, each geometry was deployed under two separate neural conditions: one with intact neurons and one with degenerated neurons that had suffered a complete loss of all peripheral processes, as exemplified by previous modeling studies (Briaire and Frijns, 2006; Kalkman et al., 2022, 2015, 2014; Snel-Bongers et al., 2013).

The model output for each simulation was presented as a threshold profile (ThP), which indicated the deterministic threshold levels of each individual neuron in the model for a given stimulus on a specific electrode contact. The single fiber thresholds were determined by iteratively simulating neural responses at different stimulus amplitudes until the highest found subthreshold amplitude was within 0.1% of the lowest obtained suprathreshold amplitude. ThPs were plotted against the nerve fiber position, which was defined by the location of the tips of the peripheral processes along the basilar membrane (BM), measured in mm from the cochlear base to the apex. ThPs were used to determine model estimates of perceptual loudness based on the total amount of space occupied at the BM by the tips of all the excited neurons. The perceptual threshold was defined in the model as the stimulus amplitude (I_{THR}) required to excite the number of fibers that corresponded to a width of 1 mm on the BM containing approximately 100 neurons (Snel-Bongers et al., 2013). The MCL in the model was defined as the amplitude (I_{MCL}) needed for an excitation width of 4 mm, which contained approximately 400 neurons (Briaire and Frijns, 2006). The difference between I_{THR} and I_{MCL} was defined as the electrical dynamic range of an electrode contact. As described by Kalkman et al. (2015), the data from the ThPs were additionally used to derive excitation density (ED) plots. ED plots indicate the percentage of neurons that are excited at a given stimulus amplitude as a function of distance along the BM. The percentage of neurons excited (i.e., the ED) at a point L along the BM was determined by calculating a moving average of neurons that had their peripheral tips located in a 1-mm segment of the BM centered on L. Accordingly, ED plots were calculated at the tip of every modeled nerve fiber, resulting in a curve of 3200 data points. The curve was smoothed with a first-order low-pass Butterworth filter. ED curves provide a rapid visualization of the differences in excitation patterns. A continuous and spatially restricted excitation region will result in a high and narrow peak on the ED curve, whereas exciting the same number of neurons in a spatially broad and discontinuous pattern will produce a wide and shallow ED peak. To investigate whether stimulation within the cochlea caused different excitation close to and remote from the facial nerve, model predictions were calculated for the stimulation of each electrode contact in all the model geometries and for both neural conditions.

2.3. Spread of excitation measurements

For the experimental part of the study, recordings were collected from 13 CI users, who were recruited at the otorhinolaryngology department of the University Hospital of Würzburg (Würzburg, Germany). The participants had to be at least 18 years old and implanted with a CI system from the manufacturer MED-EL for at least one year. Only implant types offering telemetric functionality for measuring ECAPs were included. The subjects were aged between 20 and 79 years (M = 60.31 years; SD = ±18.15). Seven subjects were implanted with a Standard and six with a FLEXsoft electrode array (for demographic details, refer to Table 1). The integrity and channel impedances of the implants were checked prior to the measurements using the clinical fitting software MAESTRO 6 (MED-EL, Innsbruck, Austria). Standard and FLEXsoft electrodes are straight electrode arrays with an active stimulation length of 26.4 mm (Dhanasingh and Jolly, 2017). The electrode array houses 12 channels, which are numbered in increasing order from the apex to the base. The Standard electrode array has two short-circuited contacts per channel, which are placed side by side at the same length. The FLEXsoft electrode array has one contact for each of the first five channels respectively and two for the remaining channels. Along their arrays, both electrode types have a spacing of 2.4 mm between channels. MED-EL CIs provide a remote reference ground electrode for stimulation and another reference contact for ECAP measurements. PULSARci100 implants have a remote ground contact on an ex-

Table 1
Demographic data of the subjects participating in the electrophysiological measurements.

Subject ID	Gender	Age [years]	Ear	Implanted [years]	Implant type	Electrode type	Etiology
S1	F	20	L	3	SYNCHRONY	FLEXsoft	Sensorineural hearing loss
S2	M	65	R	9	SONATAti100	Standard	Progressive sensorineural hearing loss
S3	F	41	R	13	PULSARci100	Standard	Progressive sensorineural hearing loss with large vestibular aqueduct syndrome
S4	F	72	L	11	PULSARci100	Standard	Unknown
S5	F	74	L	11	PULSARci100	Standard	Progressive hearing loss
S6	M	54	L	2	SYNCHRONY	FLEXsoft	Otosclerosis
S7	M	77	L	2	SNYCHRONY	FLEXsoft	Combined hearing loss with tympanosclerosis
S8	M	79	L	7	SONATAti100	Standard	Vestibulocochlear dysfunction and cholesteatoma
S9	F	58	R	3	SYNCHRONY	FLEXsoft	Congenital hearing loss and sudden hearing loss
S10	M	79	L	10	PULSARci100	Standard	Progressive hearing loss
S11	F	71	L	4	SONATAti100	FLEXsoft	Sensorineural hearing loss
S12	F	62	L	14	PULSARci100	Standard	Unknown
S13	F	32	R	7	CONCERTO	FLEXsoft	Unknown

ternal lead placed under the temporalis muscle (Bahmer et al., 2010b). More recent implant types have both reference contacts integrated in the implant housing. The experimental setup for conducting ECAP measurements was based on the one introduced by Bahmer et al. (2010a). The hardware consisted of a personal computer connected to a Research Interface Box 2 (RIB2) from the Department of Ion Physics and Applied Physics at the University of Innsbruck (Innsbruck, Austria). The stimulation and recording parameters as well as the visualization and storage of the data were controlled via a graphical user interface programmed with the software MATLAB R2017b (The MathWorks Inc., Natick, USA). During the ECAP measurements, the implant received power and commands from the RIB2 via a telemetric transmitter coil magnetically held in place above the subject's CI. The CI first converted the commands into stimulation pulses on a selected electrode contact. The subsequent ECAP response was recorded from a contact position directly apical to the stimulating contact. The recorded signal was read by the RIB2 and stored on the personal computer. To improve the signal-to-noise ratio (SNR), 50 measurement repetitions were averaged per recording. Additionally, a low-pass filter with a -3 dB drop-off at 31.5 kHz and -61 dB at 106.2 kHz was used to filter each ECAP signal. All the stimulation parameters were verified beforehand by testing the setup with a RIB detector box (MED-EL, Innsbruck, Austria) and a digital oscilloscope (Tektronix TDS 5054, Beaverton, USA). ECAP recordings always comprise electrical stimulation artifacts that can be superimposed on the electrophysiological signal of interest. Several methods have been developed to reduce the electrical stimulation artifacts in ECAP recordings, such as scaled templates (Miller et al., 1998), alternating stimulation polarity (Alvarez et al., 2007), and forward-masking methods (Abbas et al., 1999; Miller et al., 2000). Since SOE measurements after Cohen et al. (2003) have required a forward-masking paradigm to estimate the overlap of neural excitation patterns, the present study used a paradigm modified by Miller et al. (2000). The ECAP amplitudes were defined as the difference between the negative peak N1, which occurs approximately 0.2–0.4 ms after the onset of the probe stimulus (Brown et al., 2000, 1990), and the subsequent positive peak P2. The recorded signal occurring between 1.3 and 1.7 ms after the stimulus onset did not include electrophysiological responses and was therefore defined as the baseline, which was subsequently subtracted from the corresponding measurement to eliminate a direct current offset.

In Measurement I, which was a prerequisite for Measurement II (SOE measurement), the neural activation of the spiral ganglion cells by BP and TP stimulation was balanced using the respective ECAP response. To ensure the methods remained consistent with the following SOE measurements, the Miller method was also used for balancing the ECAP responses to eliminate electrical stimulation artifacts. The masker-probe interval used was 10 ms for the unmasked (Miller et al., 2001) and 0.4 ms for the masked sequence (Morsnowski et al., 2006). The BP and TP stimulation levels were adjusted to produce comparably high ECAP amplitudes for both pulse shapes. To prevent uncomfortably loud sensations during the measurements, this adjustment was performed at the most sensitive contact of each subject, namely the contact with the lowest MCL. The second column of Table 3 lists which electrode contact was used for ECAP balancing for each subject. The middle segment of Fig. 2 schematically illustrates the adjustment process. First, the masker and probe were set to the BP shape and the stimulation levels of masker and probe were successively increased in steps of 9.45 CU (the smallest possible step size in the highest current range of MED-EL implants) until the subject reported an auditory percept at the MCL. If an ECAP response was clearly visible, the experimenter noted the value of the stimulation level and the ECAP amplitude; if no ECAP was measurable at the MCL, the experiment was ended and the subject was excluded from the measurement. Second, the pulse shape and the stimulation level of the masker were kept unchanged while the shape of the probe was set to a TP and its level was decreased to zero. The biphasic masker remained the same as in the first step to minimize the parameter changes and because TPs are less effective maskers than BPs (Bahmer et al., 2010a). The stimulus level of the probe was then gradually increased until an ECAP amplitude comparable to that recorded in the first step (biphasic probe) could be measured. The adjusted TP stimulation level and the corresponding ECAP amplitude were noted.

In Measurement II, the SOEs for the BP and TP stimulations were determined. To measure the SOEs with ECAPs following the method of Cohen et al. (2003), equal stimulation levels were used on each available electrode contact of the array. The same masker-probe intervals as in Measurement I were used for Measurement II. The adjusted BP and TP stimulation levels from Measurement I were used to determine the SOE at three different probe positions. The probe positions were defined as apical (Contact Numbers 2–4), medial (Contact Numbers 5–8), and basal (Contact Numbers 9–12). SOE measurements were recorded for each subject with one apical, one medial, and one basal probe position. The electrode contacts used as the probe positions for each subject depended on which contacts were available based on the subject's audio processor fitting. Columns 3, 4, and 5 of Table 3 show which contacts were used during the SOE measurements for the probe (P) and the recording electrode (R). Comparable to Measurement I, the masker remained set to a BP while the pulse shape of the probe was either a BP or TP. Generally, the SOE measurement method

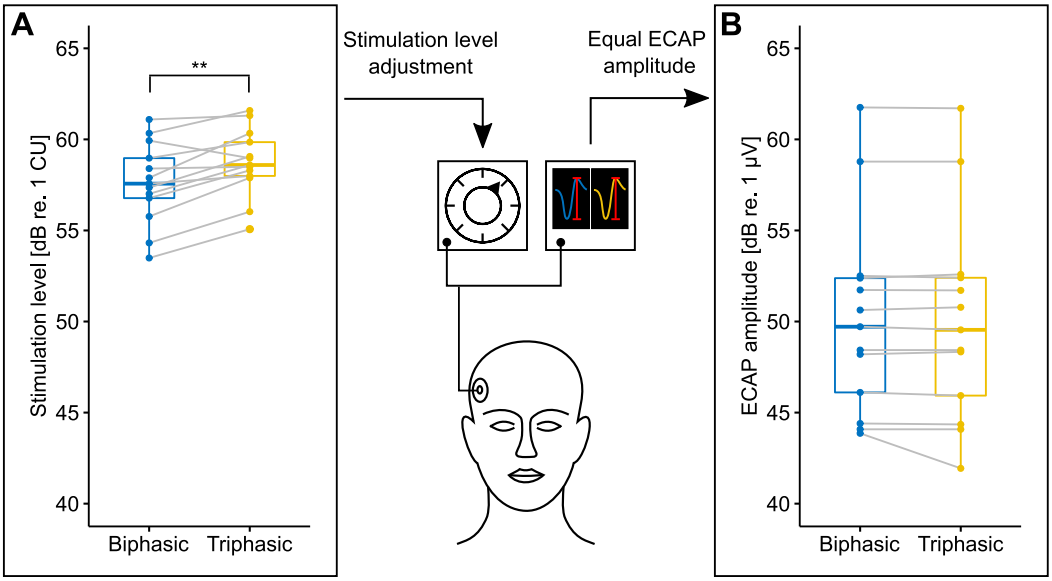

Fig. 2. Required stimulation levels (A) for equally high electrically evoked compound action potential (ECAP) amplitudes (B) after stimulation with BPs and TPs. The dots represent the results for single subjects, while the gray lines pair the results of BP and TP stimulations for the same subject. The asterisks in the left graph indicate the significant *p*-value of a non-parametric Wilcoxon signed-rank test. The center illustration depicts a schematic of the measurement procedure for the adjustment.

used results in an ECAP amplitude profile with a maximum at the position of the probe or nearby and sloping flanks towards the distant contacts. Profiles with an SNR smaller than 6 dB at the probe position were excluded from further analysis. Corresponding to Biesheuvel et al. (2016), the SNR of an ECAP was calculated as the ratio of the respective root mean square (RMS) of the signal and the noise. The signal was defined as the clearly visible electrophysiological response in the recorded data beginning after 0.2 ms and ending before 1.6 ms. The noise was defined as the signal beginning after the amplitude returned to zero (after 1.6 ms) until the end of the recording. Since ECAPs were only visually discernible from the noise above an amplitude of 50 µV, all the SOE profiles that showed a lower ECAP amplitude at the probe position were excluded. The values between contacts were calculated using linear interpolation. Each SOE profile was normalized by dividing its ECAP amplitudes by the profile's maximum value. The width of each profile was measured at the level of 25, 50, and 75% of the normalized ECAP amplitude. If the flanks of an SOE profile were not steep enough to intersect the normalized ECAP amplitude levels, the distance between the unilateral intersection and the outermost electrode contact was defined as the profile width. This approach was particularly necessary for the apical and basal probe positions as well as for the two lower normalized ECAP amplitude levels at 25 and 50%. Finally, the results were multiplied with the interelectrode distance measured in millimeters of each subject's specific electrode type.

3. Results

3.1. Model predictions

3.1.1. Threshold profiles

Fig. 3A and B illustrate the ThPs (for a description, refer to Section 2.2) for the modeled cochlear geometry CM3 as a representative of the set of all five geometries. The upper row of Fig. 3A shows the ThPs for a medial electrode contact located 284° from the round window after BP stimulation (left side) and TP stimulation (right side). The lower row comprises two magnified sections from the respective ThPs. Fig. 3B is arranged identically to Fig. 3A but depicts the ThPs for an apical electrode contact located 512° from the round window. The horizontal green and red lines indicate the amplitudes I_{THR} and I_{MCL}, respectively, which define the dynamic range (indicated by black double arrows in the bottom row of each figure). The vertical dashed line indicates the approximate location of the stimulating electrode contact.

For the medial electrode contact position (see Fig. 3A), the biphasic and triphasic stimuli produced similar single fiber threshold patterns below I_{MCL} (the area beneath the red horizontal lines), although I_{MCL} and I_{THR} were elevated for triphasic stimulation. The largest differences between the two pulse shapes occurred for fibers located more than ±3 mm from the electrode (as measured along the BM). These fiber thresholds were generally above I_{MCL}, although for the BP some of the fibers in the far apex of the cochlea were excited below that level (see the left side) due to cross-turn stimulation (Frijns et al., 2001). The TP stimulation generated higher thresholds in the apex (right side) relative to the MCL; this behavior was almost universally consistent for all the model geometries and electrode contacts. The implication is that switching from BP to TP stimulation reduces cross-turn stimulation. A ThP for a basal contact is not shown in the results of the present study as the basal ThPs were comparable to the medial ThPs in Fig. 3A, with the main site of excitation nearer to the base of the cochlea but otherwise following equivalent patterns. By contrast, the apical electrode contact position (see Fig. 3B) yielded a considerably lower I_{THR} and I_{MCL} than the basal and medial contacts but with a much smaller dynamic range. As previously, I_{THR} and I_{MCL} were both elevated for TPs (right side), relative to BPs (left side). The threshold patterns for the apical electrode contact position were much less symmetrical in the cochlear apex, showing broad shoulders on the apical side of the stimulating contact, particularly for the BPs.

3.1.2. Excitation density

Fig. 4 shows ED plots for the same cochlear geometry (CM3) and electrode configuration as the ThPs in Fig. 3A and B. The ED plots compare the neural recruitment properties of both pulse shapes. The blue curves correspond to BP simulation and yellow to TP stimulation at I_{MCL}. The first row shows predictions for the Number 6 electrode contact (medial position) and the second row for the Number 3 electrode contact (apical position). The left col-

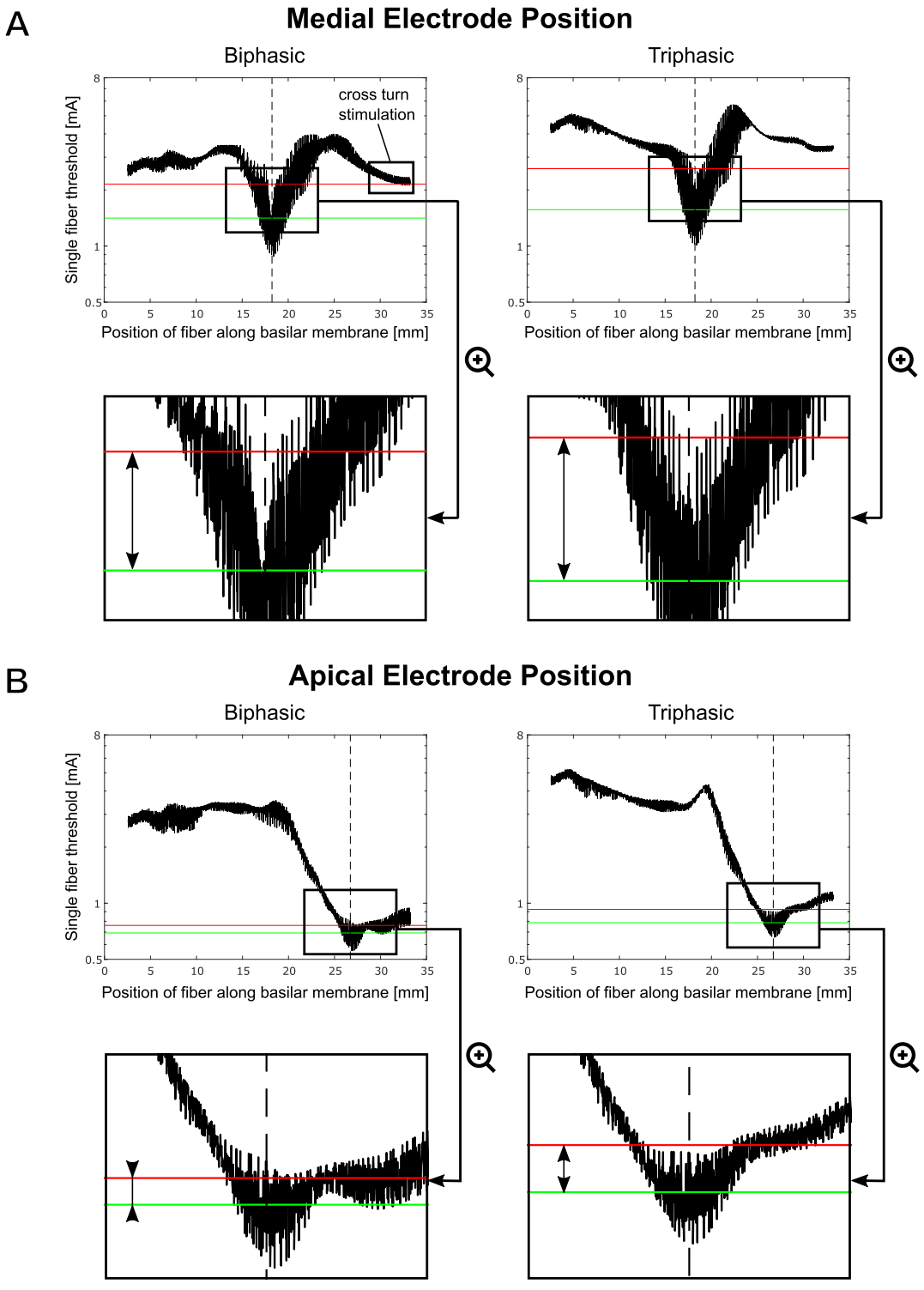

Fig. 3. Example threshold profiles for a single cochlear geometry (CM3). The threshold profiles for the BP (left side) and TP (right side) stimulation studied in the medial (A) electrode position (located 284° from the round window) and apical (B) electrode contact position (located 512° from the round window) in one of the model geometries implanted with a MED-EL Standard cochlear implant (CI) array. The ordinate indicates the single fiber threshold levels of the modeled neurons in mA, while the abscissa denotes the position of those neurons measured in mm along the basilar membrane. Black double arrows indicate the electrical dynamic range as the distance between the simulated perceptual threshold (green line) and simulated maximum comfortable loudness (red line). Vertical dashed lines indicate the approximate location of the stimulating contact. In the top row, a 5 mm wide section is marked around the position of the stimulating contact, which is magnified for better visibility in the bottom row.

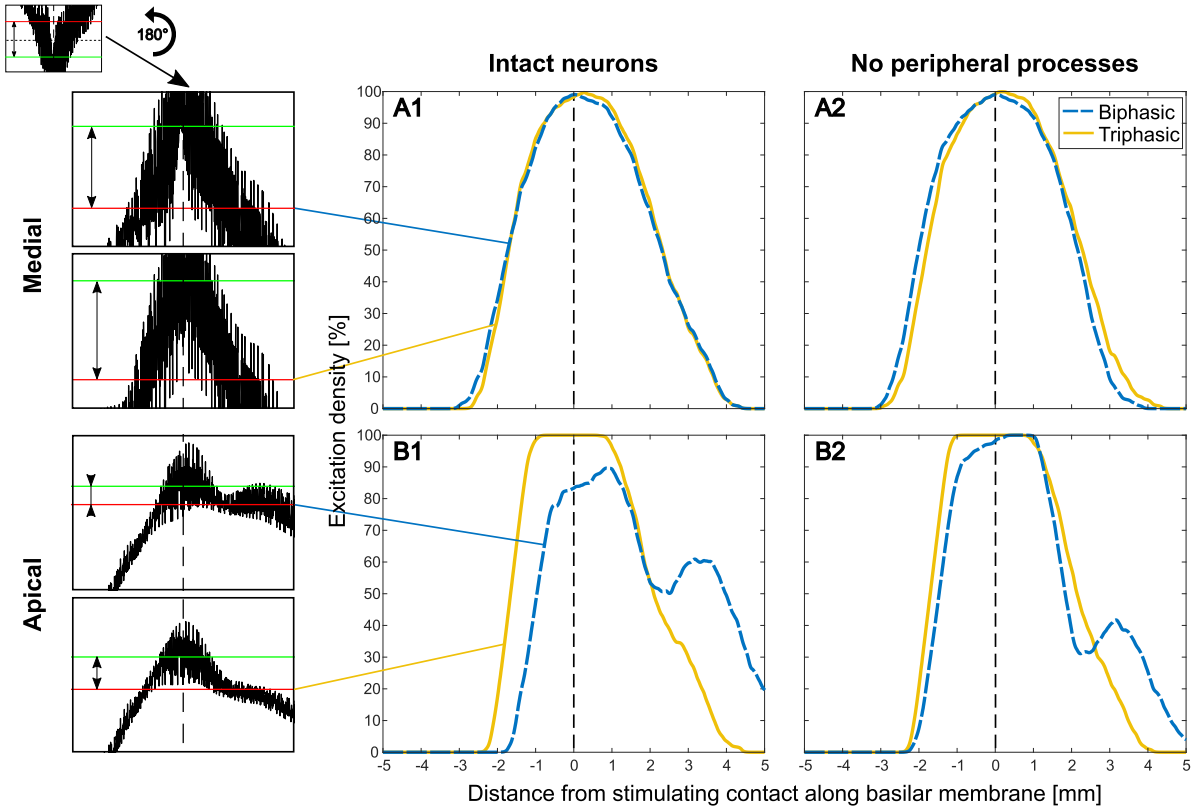

Fig. 4. Example of the excitation density (ED) plots derived from the threshold profiles of one cochlear geometry (CM3) in Fig. 3A and B. The abscissa represents the position along the basilar membrane, centered on the peak of the excitation density curves, and the ordinate represents the percentage of excited neurons in a 1 mm segment at a given position of the basilar membrane. Rows A and B correspond to a medial and apical electrode contact position on the CI array, respectively. Columns 1 and 2 show excitation density plots at the simulated most comfortable loudness with intact neurons and neurons with no peripheral processes, respectively. Excitation after stimulation is indicated with dashed blue curves for the BPs and solid yellow curves for the TPs. To the left of the ED plots for intact neurons, sections of the threshold profiles from Fig. 3 are shown rotated by 180° to illustrate their link to the ED plots.

umn contains magnified sections of the ThPs in Fig. 3A and B rotated 180° to illustrate the relationship between the ThPs and ED plots. The middle column depicts the ED curves for intact neurons and the right column for degenerated neurons with a complete loss of peripheral processes. While the ED plot for the medial contact position presents virtually identical curves for both pulse shapes with intact peripheral processes, the loss of the latter slightly shifts the curve for the BPs towards the base (Fig. 4A1 and A2). The ED curves for the basal contacts are omitted from Fig. 4 since they were again equivalent to the curves of the medial contacts. For the apical electrode contact position, the ED plots display larger differences between the BPs and TPs (Fig. 4B1 and B2). Compared to the TP stimulation ED curve, the BP curve is shallower and asymmetric due to a shoulder at the apical side of the curve, which is a result of the asymmetry seen in Fig. 3B. The largest differences between the apical ED curves of the two pulse shapes exist for neurons with intact peripheral processes (Fig. 4B1). For these neurons, the BP curve reaches its maximum at approximately 90% of the ED and its basal shoulder shows a relatively high peak of about 60%. For the degenerate neurons, both pulse shapes reach a comparably high maximum, although the BP curve is steeper and exhibits a shoulder in the apical direction. To statistically quantify the visible differences between Fig. 4B1 and B2, the RMS difference between the ED plots of the BP and TP stimulations at the MCL was calculated for all the electrode contacts in all five cochlear geometries. Fig. 5 plots these differences against the cochlear angles of the respective electrode contacts. The data points are split into basal, medial, and apical regions, indicated by the vertical dashed lines. The boundaries were based on the average contact positions of the MED-EL Standard and FLEXsoft arrays in accordance with the findings of Canfarotta et al. (2020), who reported average insertion angles of 163° and 116° for electrode contacts 8 and 9, respectively. Accordingly, the basal boundary was set at 140° in the model. For electrode contacts 4 and 5, Canfarotta et al. reported angles of 381° and 326°, so the apical boundary was set to 360° The figure clearly depicts that the RMS values in the apical region varied more than in the other two regions. As the RMS differences were not normally distributed, a Kruskal-Wallis one-way ANOVA test was used, which revealed that there was indeed a statistical difference between the cochlear regions ($p < 0.001$). Post-hoc Wilcoxon rank sum tests with Bonferroni corrections showed that the apical values were significantly different from the medial ($p = 0.004$) and basal values ($p < 0.001$) and that the medial and basal values were also significantly different from each other ($p < 0.001$). Additionally, a separate Wilcoxon rank sum test showed that there was no significant difference between the data from the intact versus degenerated neurons ($p = 0.86$). It is worth noting that a few of the outliers in the medial region could be attributed to the presence of cross-turn stimulation at the MCL for the BPs (points marked with an X). This was also related to the earlier observation that the cross-turn stimulation thresholds were higher for TP stimulation than for BP stimulation (see Section 3.1.1) since cross-turn stimulation caused the RMS values for these contacts to be higher than those of other contacts near the same cochlear angles.

3.1.3. Electrophysiological measurements

ECAP measurements contain internal noise because of the electrical amplifier. The D-trace method suggested by Hey and Müller-Deile (2015) was used for an offline N1P2 error approximation of

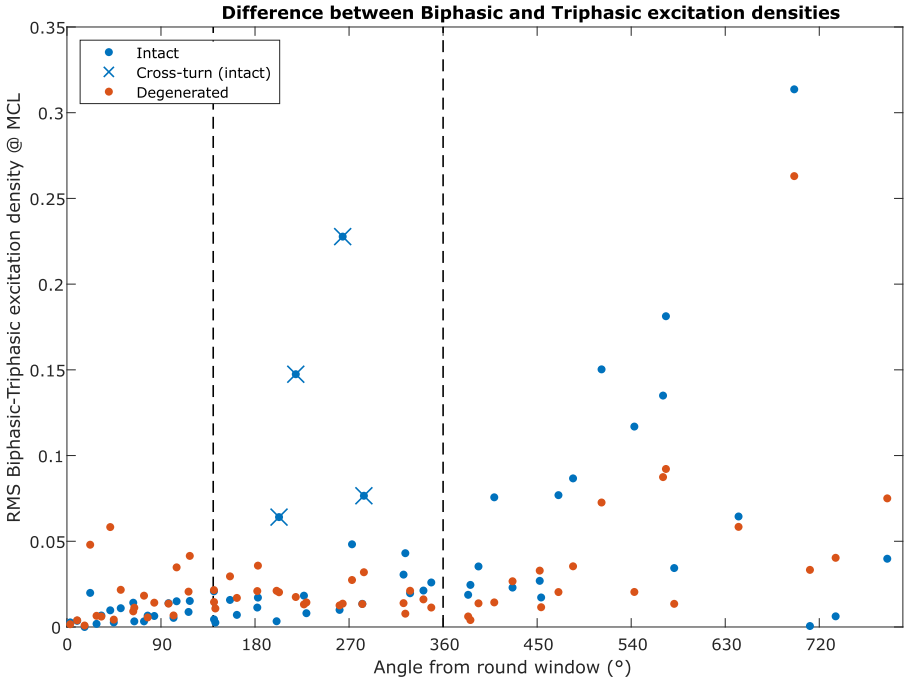

Fig. 5. Root mean square (RMS) difference between the ED plots of the BP and TP stimulations at the most comfortable loudness for all the electrode contacts in all five cochlear geometries plotted against the cochlear angles of the respective contacts. The blue dots indicate values for neurons with intact peripheral processes, the red dots show values for the degenerated condition, and blue crosses mark the presence of cross-turn stimulation.

Table 2
Datasets of subjects excluded for not meeting the inclusion criteria.

Normalized ECAP amplitude	75%	50%	25%
Apical probe	–	–	S7
Medial probe	–	–	S1, S5, S10
Basal probe	S7, S9, S10	S5, S7, S9, S10	S2, S5, S7, S9, S10

the ECAPs recorded in this study. According to that, 50 repetitions per sequence of the Miller method led to an N1P2 error of 21.12 µV. In accordance with the inclusion criteria defined in Section 2.3, the basal recordings of subjects S7, S9, and S10 had to be excluded from the analysis. Furthermore, not all the SOE profiles of the included subjects showed a measurable profile width at each probe position and a normalized ECAP amplitude. If a quantifiable profile width was determined for only one of the two pulse shapes, both datasets were excluded to avoid bias. Table 2 summarizes the datasets excluded from the analysis.

Measurement I: Stimulation level adjustment: An increase in the stimulation level from the BP to the TP was required for all but one subject (see Fig. 2A) to gain an equally high ECAP response (see Fig. 2B). A non-parametric Wilcoxon signed-rank test ($\alpha = 0.05$) showed a significant difference between both pulse shapes for the stimulation levels ($W = 5$, $p < 0.01$) and a non-significant difference between the ECAP amplitudes ($W = 35$, $p = 0.476$). The median TP stimulation level was 1.023 dB re. 1 CU higher than the median of the BP stimulation.

Measurement II: Determination of SOE profile widths: SOE profiles were measured at an apical, medial, and basal probe position for the BP and TP stimulations. The ECAP amplitudes of each SOE profile were normalized to the maximum of each profile. Fig. 6 depicts these results. For each measurement condition (probe position x pulse shape), the mean of all the normalized ECAP amplitudes per electrode contact (shown as a black line) was calculated, provided that at least three measurement points were obtained. Measurement points were missing if either the electrode contacts in the subject's fitting map were deactivated because of unpleasant perceptions and consequently not used for the measurement or if the electrode contacts were used as recording electrodes during the measurement. Table 3 describes which electrodes were deactivated or used as recording electrodes. The mean per-pulse shape exhibits the typical SOE profile shape for the medial probe position with two flanking slopes: one steep to the base of the cochlea and the other shallow towards the apex. The mean of the SOE profiles for the apical and basal probe positions demonstrate only one slope. The apical slope descends constantly towards the base, while the basal slope has a steep and flat segment in the direction of the apex. The variability for the BP and TP curves appears visibly similar for the apical, medial, and basal probe positions (see Fig. 6). Due to the normalization, the visual variability decreases in the direction of the respective maximum, which in most cases occurs at the probe position. A repeated-measures three-way analysis of variance (ANOVA) was performed to examine the effects of the pulse shape, the position of the probe, and the level of the normalized ECAP amplitude on the SOE profile width, treating the subject as a random effect. In order to create a data set of only complete pairs of profiles widths, the subjects S5, S7, S9, and S10 as well as the complete level of 25% normalized ECAP had to be excluded from analysis. Fig. 7 consists of three box plot diagrams that compare the SOE profile widths of the BP and TP stimulations for the apical, medial, and basal probe positions that were included in the ANOVA. Each diagram compares the profile widths for 50 and 75% of the normalized ECAP amplitude. While the medial and basal probe positions show the widest and narrowest SOE, respectively, each probe position indicates a stepwise decline of the SOE profile width from 50 to 75% of the normalized ECAP amplitude. The dis-

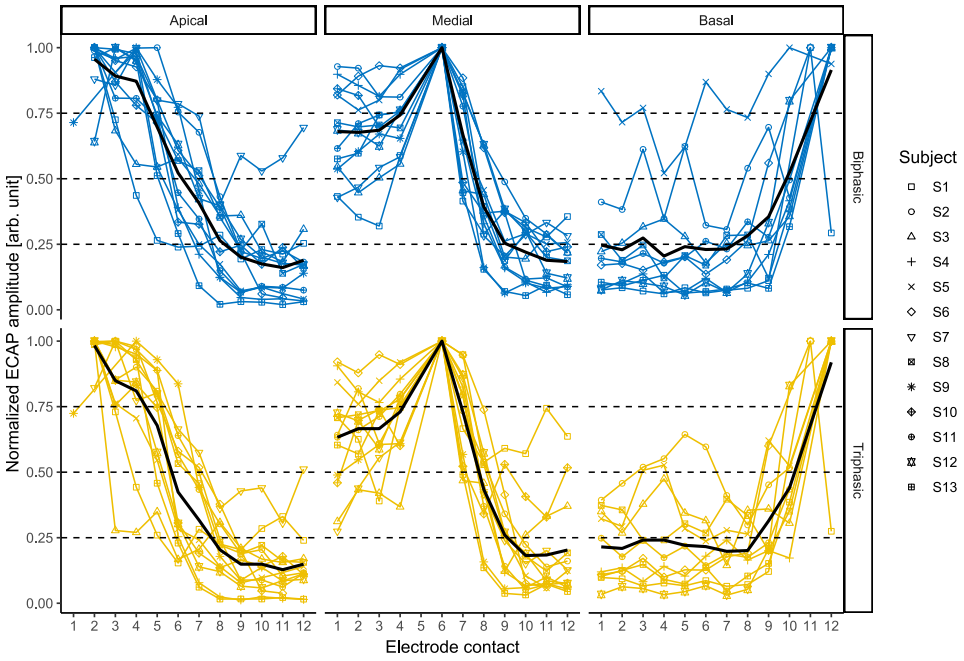

Fig. 6. Spread of excitation (SOE) profiles for the BP and TP stimulations at the apical, medial, and basal probe positions. The abscissa represents the electrode contact number of the masker stimulus. The ordinate represents the ECAP amplitude normalized to each profile's respective maximum value. The colored lines depict the linearly interpolated SOE profiles for each subject and pulse shape (blue: BP; yellow: TP). The measurement points of each subject can be distinguished by subject-specific symbols. The black line indicates the mean value of all the normalized ECAP amplitudes of the respective measuring condition, assuming that there were at least three measuring points for the respective electrode contact. The dashed horizontal lines indicate 25, 50, and 75% of the normalized ECAP amplitude.

Table 3
Electrode contacts used to balance biphasic and triphasic ECAP amplitudes in Measurement I and electrode contacts used as a probe (P) or recording electrode (R) during the SOE measurements in Measurement II.

Subject ID	Deactivated electrode contacts in processor fitting	Electrode contact used for balancing ECAP amplitudes	Electrode contact used for recording (R) and as probe (P)		
			Apical	Medial	Basal
S01	–	11	R1P2	R5P6	R10P11
S02	–	1	R1P2	R5P6	R11P12
S03	–	4	R1P2	R5P6	R11P12
S04	–	1	R1P2	R5P6	R11P12
S05	–	3	R1P2	R5P6	R11P12
S06	–	11	R1P2	R5P6	R10P11
S07	–	8	R1P2	R5P6	R11P12
S08	–	3	R1P2	R5P6	R11P12
S09	2	1	R3P4	R5P6	R11P12
S10	–	2	R1P2	R5P6	R11P12
S11	–	2	R1P2	R5P6	R11P12
S12	–	3	R1P2	R5P6	R11P12
S13	–	2	R1P2	R5P6	R11P12

tribution of the ANOVA's residuals was tested for normality using a Kolmogorov-Smirnov test ($\alpha = 0.05$) and showed a significant deviation from a normal distribution ($D = 0.153$, $p < 0.05$). Therefore, the results of the parametric ANOVA were rejected and a non-parametric repeated-measures three-way aligned-rank transformed (ART) ANOVA (Wobbrock et al., 2011) was performed instead using the same inputs as for the parametric ANOVA. The results showed no significant main effect of the pulse shape, $F(1, 88) = 0.301$, $p < 0.05$. The main effect of the probe position was significant, $F(2, 88) = 153.49$, $p < 0.001$ and the main effect of the level of the normalized ECAP amplitude was significant, $F(1, 88) = 79.945$, $p < 0.001$. The interaction effect between the pulse shape and the probe position was not significant, $F(2, 88) = 0.738$, $p < 0.05$ and the interaction effect between the pulse shape and the normalized ECAP amplitude level was not significant, $F(1, 88) = 0$, $p < 0.05$. The interaction effect of the probe position and the normalized ECAP amplitude level was significant, $F(2, 88) = 13.666$, $p < 0.001$, while the interaction effect of all three independent variables was not significant, $F(2, 88) = 1.116$, $p > 0.05$. The main effect of the probe position was to be expected, since for a medial position the SOE profiles expand apically and basally from the centrally located probe. In contrast, the SOE profiles for the apical and basal probe positions can only expand in the basal and apical direction, respectively. Because of this, approximately only half of the SOE profile is acquired for the apical and basal probe positions. As a consequence, the width of the apical and basal SOE profile were expected to be narrower than the medial profile. Similarly, the main effect of normalized ECAP amplitude level was to be expected, since SOE profiles measured with the Miller method generally exhibit a peak at the position of the probe with sloping flanks towards apex and basis. Thus, the cross-section of a SOE profile at 50% (i.e., closer to the base of the profile) always shows a broader width than at 75% (i.e., close to the peak of the profile). Because the focus of this study was on the main of the pulse shape and its interaction effects, no post hoc tests were performed to examine the main effects of probe position and normalized ECAP amplitude level and the interaction between them.

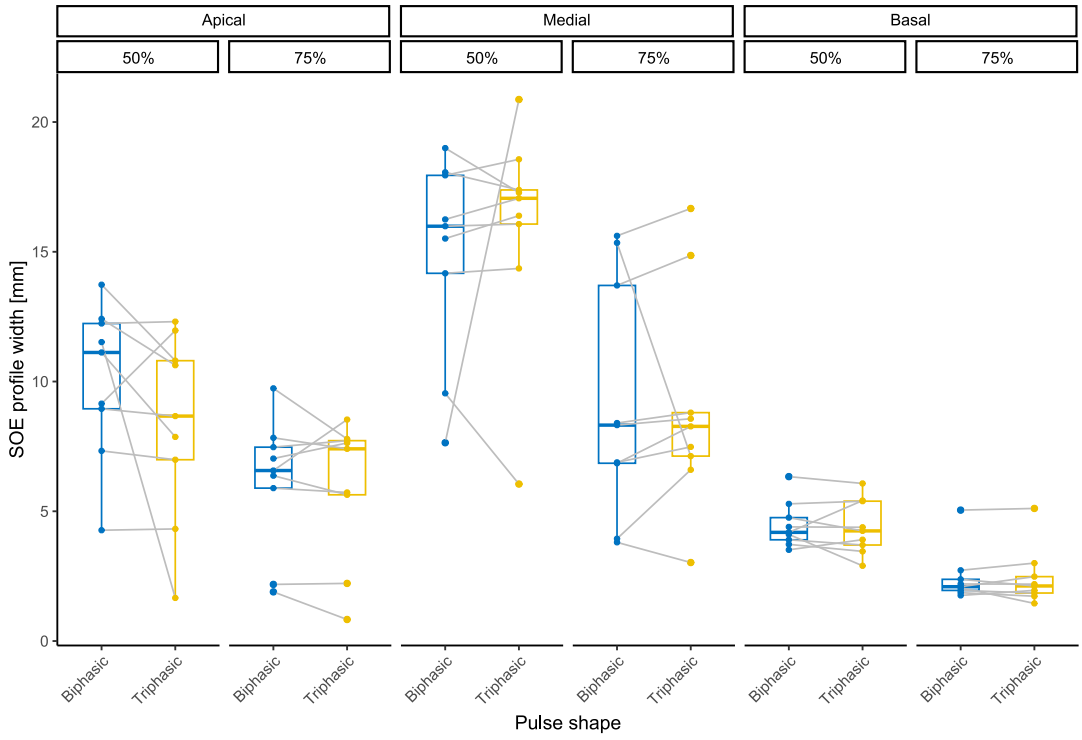

Fig. 7. Paired comparison of the biphasic- and triphasic-stimulated SOE profile widths for the apical, medial, and basal probe positions. The box plots compare the SOE profile widths (ordinate) at two different levels of the normalized ECAP amplitude (i.e., 50 and 75%). All compared SOE profile widths are arranged in pairs of BPs and TPs. For each pair, the results of the BPs (blue) are shown on the left and of the TPs (yellow) on the right (comparable to Fig. 2).

The ECAP amplitudes after the BP and TP stimulations at the probe position for the apical, medial, and basal test sites were compared. To ensure consistency in the comparison, subjects were excluded whose probe positions did not correspond to electrode contacts 2, 6, and 12 or for whom no dataset was measured for one of the test sites. Accordingly, subjects S6, S7, S9, and S10 were excluded. A repeated-measures two-way ANOVA test was performed to evaluate the effect of the pulse shape at the different test sites on the ECAP amplitude. A Shapiro-Wilk test revealed that the residuals of the ANOVA did not deviate significantly from normality ($W = 0.98$, $p < 0.05$). There was no statistically significant two-way interaction between the pulse shape and test site, $F(2, 16) = 0.104$, $p < 0.05$, and no significant main effect of the pulse shape, $F(1, 8) = 1.546$, $p < 0.05$. However, there was a statistically significant main effect of the test site, $F(2, 16) = 10.59$, $p < 0.01$. Therefore, the effect of the test site was analyzed using a paired t-test ($\alpha = 0.05$). The p-values were adjusted using Bonferroni's correction for multiple testing. Fig. 8 depicts the ECAP amplitudes from the apical, medial, and basal test site as box plots together with the results of the paired t-test indicated as asterisks above the respective pair of test sites. The pairwise comparison showed that ECAP amplitudes measured in the apical test site ($M = 50.539$; $SD = 6.159$) were significantly larger than those in the medial test site ($M = 47.254$; $SD = 5.624$), $t(17) = 4.8$, $p < 0.001$. The apical ECAP amplitudes were also significantly larger than those in the basal test site ($M = 43.621$; $SD = 5.956$), $t(17) = 5.031$, $p < 0.001$. Moreover, the medial ECAP amplitudes were significantly larger than the basal amplitudes, $t(17)$, $p < 0.05$.

4. Discussion

This study systematically evaluated which intracochlear processes potentially contribute to the FNS reduction by TP stimulation compared to BP stimulation. The evaluation consisted of auditory nerve responses to BPs and TPs simulated in a computational model of the human cochlea and electrophysiological measurements of the SOEs in CI users.

4.1. Equal electrically evoked compound action potential amplitudes require higher levels for triphasic pulse than biphasic pulse stimulations

For most of the subjects, the stimulation level had to be increased during the measurement by 1.023 dB re. 1 CU to match the ECAP amplitudes for the BP and TP stimulations (Fig. 2). This result accords with the findings of previous studies, which demonstrated that to match the psychophysical loudness, the TP stimulation level had to be increased compared to the BP stimulation level despite an equal charge (Bahmer et al., 2010b; Bahmer and Baumann, 2013; Herrmann et al., 2021). Although electrophysiological peripheral measurements do not necessarily reflect psychophysical measurements, ECAP amplitudes may reflect an initial approximation for loudness. The results exhibited a notable consistency between subjects; therefore, a strong influence of individual physiological properties can be excluded. Furthermore, this electrophysiological adjustment to a constant ECAP amplitude as a prerequisite of the subsequent SOE measurements was robust. This robustness avoided the high variability typical of psychophysical tests.

4.2. Comparison between simulated neural responses and experimental measurements

Compared to the SOE measurements of CI users, the computational model has the advantages that its results can direct the focus to a certain effect and that its spatial resolution can be chosen freely. The clear difference between the BP and TP stimulations, which appeared towards the apical region of the modeled

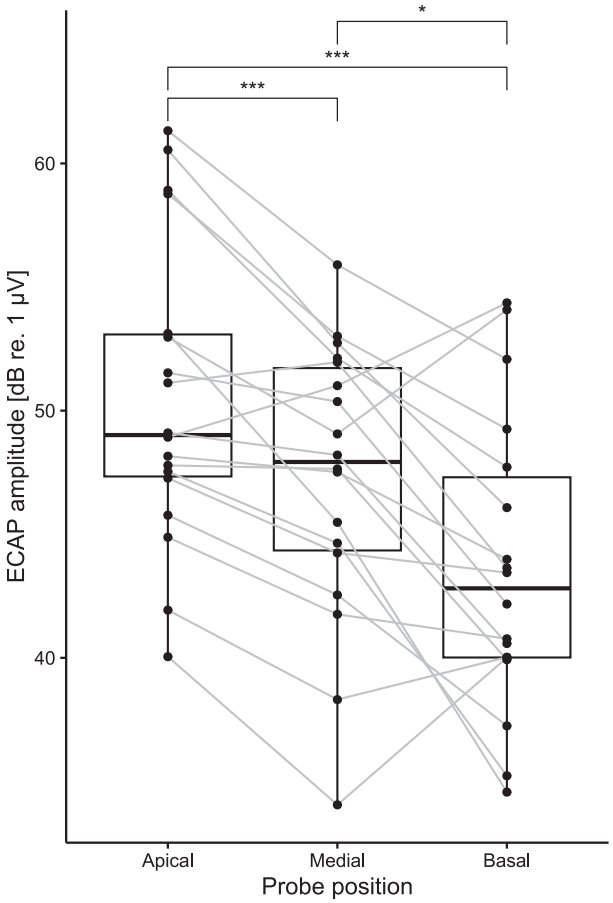

Fig. 8. ECAP amplitudes measured at the apical, medial, and basal probe position. Each box plot corresponds to one of the probe positions and integrates the responses to BP- and TP-stimulation. The dots represent the results for single subjects, while the gray lines connect the ECAP amplitudes of each test site for the same subject. A paired *t*-test of the ECAP amplitudes revealed significant difference between all test locations (indicated as asterisks above each comparison). The *p*-values were adjusted using the Bonferroni's correction for multiple comparisons.

cochlear geometries, motivated the SOE measurements in different cochlear regions. However, no differences were detected between the biphasic and triphasic stimulated SOEs using the electrophysiological measurements.

In the model results shown in Figs. 3 and 4, apical stimulation with the BP led to a prominent secondary site of stimulated nerve fibers 3.5 mm further along the BM in the apical direction from the main excitation area near the stimulating electrode contact. Closer inspection of the data revealed that this secondary area of excitation occurred in the central axons of neurons whose peripheral processes terminate roughly half a cochlear turn apically from the position of the stimulating contacts, a phenomenon identified in previous modeling studies and referred to as cross-turn stimulation (Briaire and Frijns, 2000a; Frijns et al., 2001, 1995; Kalkman et al., 2022, 2014). The central axons of these neurons were located near the central axons of the neurons belonging to the primary site of excitation due to the way the spiral ganglion terminates in the apex of the cochlea (Kalkman et al., 2014). The modeling data revealed that the threshold for stimulating neurons associated with more apical cochlear (half) turns was almost invariably lower for the BP than for the TP (data not shown). This may be reflected in the significantly higher stimulation levels that were required in Measurement I to match the ECAP responses of TP to BP stimulation. Experimental results from previous studies have indicated a higher efficacy of anodic stimulation compared to cathodic stimulation in the activation of human ANFs (Macherey et al., 2008; Undurraga et al., 2010). Although previous modeling work has indicated that anodic stimulation predominantly activates the central axons of ANFs, while cathodic stimulation targets the neuron's peripheral processes or near their somata (Joshi et al., 2017; Potrusil et al., 2020; Rattay, 1999; Rattay et al., 2001b, 2001a; Resnick et al., 2018), it should be noted that this mainly applies to same-turn stimulation. For neurons originating in other turns of the cochlea, recent modeling work suggests that the central axons tend to be more sensitive to cathodic stimulation (Kalkman et al., 2022), as was reflected in the secondary cross-turn sites of excitation in the present study's apical contact stimulation modeling results. This information is the key to understanding the differences between BPs and TPs in Fig. 4B1 and B2; splitting the cathodic phase into two shorter and therefore less effective cathodic phases caused the central anodic phase of the TPs to become the more dominant phase of the pulse. Consequently, the decreased effectiveness of the cathodic phases of the stimulus reduced the cross-turn stimulation of the TP in the apex of the cochlea relative to the BP, which is why the triphasic ED plots in Fig. 4B1 and B2 do not show the prominent apical secondary peaks present in the equivalent BP curves.

The model was also used to study the responses of neurons without peripheral processes to mimic the effect of neural degeneration. The effect of degeneration was weak compared to the effect of stimulation with different pulse shapes. For the medial contact position, the simulated degeneration slightly shifted the responses towards the apex. A similar shift occurred for the apical contact; however, in this region a large difference between the BP and TP stimulations could be observed, due to the fact that the cathodic phase of the BP excites some of the neurons in the peripheral processes (if they are present), whereas the TP stimulates almost exclusively in the central axons.

SOE measurements were performed with an apical, medial, and basal probe position. On average, the ECAP absolute response amplitudes increased from the basal to the apical contact. This change could be attributable to both the electrode-modiolus distance, which decreases from the cochlear base to the apex (Brill et al., 2009; Medina et al., 2013), and to the higher density of neurons in the upper basal turn (Spoendlin, 1972). The lower ECAP amplitudes stimulated by contacts near the cochlear base resulted in a lower SNR, which in turn made it difficult to collect meaningful SOE profiles for the basal probe position. Especially at the low normalized ECAP level of 25%, this made it impossible to determine a profile width for a number of subjects, resulting in the exclusion of four subjects and the complete level of 25% from analysis. Subtle differences, which are visible in the simulation, could be masked by a low SNR in the SOE measurements, for example at the basal probe position (Biesheuvel et al., 2018). The ART ANOVA showed no effect of the pulse shape on the SOE profile width. A possible reason for this could be the small sample size, which was further reduced by excluding data sets with low SNR. Thus, a possibly existing but small effect of the pulse shape could not be detected. However, this result aligns with the results of Bakhos et al. (2013), who used similar pulse shapes in SOE measurements.

Since the modeled and experimental results in the present study showed no consistencies, it is important to note the differences between both approaches. SOE profiles result from the overlap of excitation patterns of multiple masker pulses and a locally fixed probe pulse. To resolve the SOE readout, the method introduced by Cohen et al. (2003) assumes uniform excitation patterns from each electrode contact, which assumption may be an oversimplification (Garcia et al., 2021). Biesheuvel et al. (2016) proposed that the SOE procedure rather corresponds to a convolution of the areas excited by the masker and the probe than the excitation the probe itself. They demonstrated that deconvolution can

be used to recover the actual excited areas. By iteratively adjusting the excitation density profiles of the masker and the probe, they were able to fit predicted SOE profiles to those measured in CI users. From the predicted excitation density profiles, they concluded that the asymmetry in SOE profiles (as observed for the medial probe position in Fig. 6 of the present study) is a consequence of the excitation in the apical part of the cochlea being wider than in the basal part. Cosentino et al. (2015) introduced the panoramic ECAP (PECAP) method to account for the fact that ECAP amplitudes reflect the joint neural activation pattern of both masker and probe activation patterns, and not just the spread of neural excitation evoked by the probe alone. It was shown that this method is suitable to detect cross-turn stimulation. Furthermore, a recent study by Garcia et al. (2021) demonstrated the ability of a revised version of the PECAP method to provide estimates of the current spread and the neural health for individual patients. The neural health estimate enabled the identification of simulated dead regions in CI patients and to correctly attribute these to local reductions in neural responsiveness, as opposed to changes in current spread. However, compared to conventional SOE measurements, the PECAP method requires ECAPs to be measured for all combinations of probe and masker locations and additional optimization algorithms. This stipulation would have required the subject in the present study to be available for a significantly longer period. Unfortunately, this was not possible as the subjects were recruited from the clinical routine. While, the conventional SOE method used in the present study represents a well-established and rapid procedure to gain an estimate of the spatial neural excitation in CI users its resolution to uncover small differences seems limited.

In contrast to the SOE recordings, the modeled ED plots represent the neural excitation patterns of individual electrode contacts rather than the convolutions of the masker and probe electrodes. Although these curves cannot be compared to the SOE data directly, they provide useful insights into the neural excitation patterns that underlie a forward-masking paradigm. Simulating ECAP recordings directly is technically also possible in the model (Briaire and Frijns, 2005), but it was computationally too time consuming to apply to this study. Furthermore, a known shortcoming of this and similar models is that predicted stimulus levels are unreasonably high compared to clinical data (Kalkman et al., 2016). In consequence, it would have been challenging to directly compare any simulated SOE recordings to data from CI subjects. Arguably, the ED plots share this problem, since the model definition of the MCL is arbitrary and it is unknown whether the number of excited model neurons at this level accurately reflects the number of neurons stimulated in real life subjects. However, increasing or decreasing the excitation width for the MCL by 1 mm (corresponding to roughly 100 more or fewer excited neurons in the model) did not change the model results to an extent that would have affected the study conclusions (data not shown). This fact provides some degree of confidence that the simulated MCL is an appropriate stimulus level to compare to the levels used in the CI subjects. In addition, efforts to deconvolve SOE data into the individual contributions of the masker and probe electrodes have revealed that the SOE data can be accurately described by assuming underlying functions that resemble and behave similarly to the ED plots from the model of this study (Biesheuvel et al., 2022, 2016).

To summarize, the computational model and ECAP measurements represent two different approaches to approximate actual intracochlear neuronal excitation, both methods bear a degree of uncertainty, which could explain the different results of both methods. Nevertheless, considering the results of computational models and electrophysiological methods together is helpful to understand the underlying intracochlear difference between BP and TP stimulations.

4.3. Future prospects

The SOE measurement had a limited resolution and could not uncover the difference found in the model simulations. Conventional SOE measurements using forward-masking paradigms can be distorted due to a non-uniform excitation density evoked by the masker and probe (Biesheuvel et al., 2016). By using the deconvolution method introduced by Biesheuvel et al. (2022, 2016), a future study could identify the influences of intracochlear stimulation site and stimulus level to further investigate the potentially existing difference between BP and TP stimulation in CI users. Another possibility to overcome the limitations of forward-masking paradigms could be using the PECAP method (Cosentino et al., 2015; Garcia et al., 2021). This method may be more sensitive to subtle and location-specific differences between neural excitation patterns after BP and TP stimulations than the SOE method applied in the present study. Garcia et al. (2022) recently described a method for multi-electrode ECAP measurements that can accelerate the otherwise time consuming PECAP method in subject recordings. As explained in the introduction, effects outside the cochlea may play a major role in the ameliorative effect of TPs on FNS. A previous study that performed electromyographic measurements of the facial nerve effector muscles of CI recipients supports the hypothesis that stimulation pulse shape and polarity strongly affects FNS (Bahmer et al., 2017). Therefore, a future study could compare the responses of facial nerve fibers and ANFs stimulated by an intracochlearly implanted electrode to further elucidate the thresholds of both nerve types for stimulations with pulse shapes of different temporal polarity distributions.

5. Conclusions

- The model predictions showed differences in the neural responses of ANFs to BP versus TP stimulation towards the cochlear apex.
- For a comparison with the model predictions, stable SOE measurements were established by referencing a constant ECAP amplitude.
- In contrast to the model, the SOE measurements could not detect significant intracochlear differences in the neural responses of the ANFs to BP versus TP stimulation.
- The modeling results imply that this difference between apical BP and TP stimulations is due to the reduced cross-turn stimulation resulting from a diminished efficacy of the shorter cathodic phases of the triphasic stimulus relative to the biphasic equivalent.

Disclosure

This study was funded by a grant of the Deutsche Forschungsgemeinschaft (DFG, BA 4237/3-1).

Data Availability

Data will be made available on request.

CRediT authorship contribution statement

David P. Herrmann: Data curation, Project administration, Visualization, Writing – original draft. **Randy K. Kalkman:** Conceptualization, Visualization, Writing – original draft, Writing – review & editing. **Johan H.M. Frijns:** Conceptualization, Writing – review & editing. **Andreas Bahmer:** Conceptualization, Funding acquisition, Methodology, Software, Writing – review & editing, Supervision.

Acknowledgments

We would like to thank the subjects for their willingness to participate in the experimental tests of this study. All the experiments with test subjects were performed in accordance with the declaration of Helsinki and under the authorization of the ethics committee of the University of Würzburg (315/15_z).

References

Abbas, P.J., Brown, C.J., Shallop, J.K., Firszt, J.B., Hughes, M.L., Hong, S.H., Staller, S.J., 1999. Summary of results using the nucleus CI24M implant to record the electrically evoked compound action potential. Ear Hear. 20, 45–59.

Alhabib, S.F., Abdelsamad, Y., Yousef, M., Alzhrani, F., 2020. Performance of cochlear implant recipients fitted with triphasic pulse patterns. Eur. Arch. Otorhinolaryngol. doi:10.1007/s00405-020-06382-0.

Alvarez, I., de la Torre, A., Sainz, M., Roldan, C., Schoesser, H., Spitzer, P., 2007. Generalized alternating stimulation: a novel method to reduce stimulus artifact in electrically evoked compound action potentials. J. Neurosci. Methods 165, 95–103. doi:10.1016/j.jneumeth.2007.05.028.

Bahmer, A., Adel, Y., Baumann, U., 2017. Preventing facial nerve stimulation by triphasic pulse stimulation in cochlear implant users: intraoperative recordings. Otol. Neurotol. 38, e438–e444. doi:10.1097/MAO.0000000000001603.

Bahmer, A., Baumann, U., 2016. The underlying mechanism of preventing facial nerve stimulation by triphasic pulse stimulation in cochlear implant users assessed with objective measure. Otol. Neurotol. 37, 1231–1237. doi:10.1097/MAO.0000000000001156.

Bahmer, A., Baumann, U., 2013. Effects of electrical pulse polarity shape on intra cochlear neural responses in humans: triphasic pulses with cathodic second phase. Hear. Res. 306, 123–130. doi:10.1016/j.heares.2013.10.001.

Bahmer, A., Peter, O., Baumann, U., 2010a. Recording and analysis of electrically evoked compound action potentials (ECAPs) with MED-EL cochlear implants and different artifact reduction strategies in Matlab. J. Neurosci. Methods 191, 66–74. doi:10.1016/j.jneumeth.2010.06.008.

Bahmer, A., Polak, M., Baumann, U., 2010b. Recording of electrically evoked auditory brainstem responses after electrical stimulation with biphasic, triphasic and precision triphasic pulses. Hear Res 259, 75–85. doi:10.1016/j.heares.2009.10.003.

Bakhos, D., Mertens, G., Van De Heyning, P., Landsberger, D.M., 2013. Effect of triphasic and biphasic pulse shapes on the spread of excitation. In: Proceedings of the Conference on Implantable Auditory Prostheses CIAP, Granlibakken Conference Center. Lake Tahoe, CA.

Battmer, R., Pesch, J., Stover, T., Lesinski-Schiedat, A., Lenarz, M., Lenarz, T., 2006. Elimination of facial nerve stimulation by reimplantation in cochlear implant subjects. Otol. Neurotol. 27, 918–922. doi:10.1097/01.mao.0000235374.85739.c6.

Berrettini, S., Vito de, A., Bruschini, L., Passetti, S., Forli, F., 2011. Facial nerve stimulation after cochlear implantation: our experience. Acta Otorhinolaryngol. Ital. 31, 11–16.

Biesheuvel, J.D., Briaire, J.J., Frijns, J.H.M., 2018. The precision of eCAP thresholds derived from amplitude growth functions. Ear Hear. 39, 701–711. doi:10.1097/AUD.0000000000000527.

Biesheuvel, J.D., Briaire, J.J., Frijns, J.H.M., 2016. A novel algorithm to derive spread of excitation based on deconvolution. Ear Hear. 37, 572–581. doi:10.1097/AUD.0000000000000296.

Biesheuvel, J.D., Briaire, J.J., Kalkman, R.K., Frijns, J.H.M., 2022. The effect of stimulus level on excitation patterns of individual electrode contacts in cochlear implants. Hear. Res., 108490 doi:10.1016/j.heares.2022.108490.

Bigelow, D., Kay, D., Rafter, K., Montes, M., Knox, G., Yousem, D., 1998. Facial nerve stimulation from cochlear implants. Am. J. Otol. 19, 163–169.

Braun, K., Walker, K., Surth, W., Lowenheim, H., Tropitzsch, A., 2019. Triphasic pulses in cochlear implant patients with facial nerve stimulation. Otol. Neurotol. 40, 1268–1277. doi:10.1097/MAO.0000000000002398.

Briaire, J.J., Frijns, J.H.M., 2006. The consequences of neural degeneration regarding optimal cochlear implant position in scala tympani: a model approach. Hear. Res. 214, 17–27. doi:10.1016/j.heares.2006.01.015.

Briaire, J.J., Frijns, J.H.M., 2005. Unraveling the electrically evoked compound action potential. Hear. Res. 205, 143–156. doi:10.1016/j.heares.2005.03.020.

Briaire, J.J., Frijns, J.H.M., 2000a. Field patterns in a 3D tapered spiral model of the electrically stimulated cochlea. Hear. Res. 148, 18–30. doi:10.1016/S0378-5955(00)00104-0.

Briaire, J.J., Frijns, J.H.M., 2000b. 3D mesh generation to solve the electrical volume conduction problem in the implanted inner ear. Simul. Pract. Theory 8, 57–73. doi:10.1016/S0928-4869(00)00007-0.

Brill, S., Muller, J., Hagen, R., Moltner, A., Brockmeier, S.J., Stark, T., Helbig, S., Maurer, J., Zahnert, T., Zierhofer, C., Nopp, P., Anderson, I., Strahl, S., 2009. Site of cochlear stimulation and its effect on electrically evoked compound action potentials using the MED-EL standard electrode array. Biomed. Eng. Online 8. doi:10.1186/1475-925x-8-40.

Brown, C.J., Abbas, P.J., Gantz, B., 1990. Electrically evoked whole-nerve action potentials: data from human cochlear implant users. J. Acoust. Soc. Am. 88, 1385–1391. doi:10.1121/1.399716.

Brown, C.J., Hughes, M.L., Luk, B., Abbas, P.J., Wolaver, A., Gervais, J., 2000. The relationship between EAP and EABR thresholds and levels used to program the nucleus 24 speech processor: data from adults. Ear Hear. 21, 151–163. doi:10.1097/00003446-200004000-00009.

Brummer, S.B., Turner, M.J., 1977. Electrochemical considerations for safe electrical stimulation of the nervous system with platinum electrodes. IEEE Trans. Biomed. Eng. 24, 59–63. doi:10.1109/TBME.1977.326218.

Canfarotta, M.W., Dillon, M.T., Buss, E., Pillsbury, H.C., Brown, K.D., O'Connell, B.P., 2020. Frequency-to-place mismatch: characterizing variability and the influence on speech perception outcomes in cochlear implant recipients. Ear Hear. 41, 1349–1361. doi:10.1097/AUD.0000000000000864.

Cohen, L.T., Richardson, L.M., Saunders, E., Cowan, R.S., 2003. Spatial spread of neural excitation in cochlear implant recipients: comparison of improved ECAP method and psychophysical forward masking. Hear. Res. 179, 72–87. doi:10.1016/s0378-5955(03)00096-0.

Cosentino, S., Gaudrain, E., Deeks, J., Carlyon, R., 2015. Multistage nonlinear optimization to recover neural activation patterns from evoked compound action potentials of cochlear implant users. IEEE Trans. Biomed. Eng. 1. doi:10.1109/TBME.2015.2476373, -1.

Crew, J.D., Galvin, J.J., Fu, Q.J., 2012. Channel interaction limits melodic pitch perception in simulated cochlear implants. J. Acoust. Soc. Am. 132, El429–El435. doi:10.1121/1.4758770.

Dekker, D.M., Briaire, J.J., Frijns, J.H.M., 2014. The impact of internodal segmentation in biophysical nerve fiber models. J. Comput. Neurosci. 37, 307–315.

Dhanasingh, A., Jolly, C., 2017. An overview of cochlear implant electrode array designs. Hear. Res. 356, 93–103. doi:10.1016/j.heares.2017.10.005.

Dorman, M.F., Loizou, P.C., Rainey, D., 1997. Speech intelligibility as a function of the number of channels of stimulation for signal processors using sine-wave and noise-band outputs. J. Acoust. Soc. Am. 102, 2403–2411. doi:10.1121/1.419603.

Frijns, J.H.M., Briaire, J.J., Grote, J.J., 2001. The importance of human cochlear anatomy for the results of modiolus-hugging multichannel cochlear implants. Otol. Neurotol. Off. Publ. Am. Otol. Soc. Am. Neurotol. Soc. Eur. Acad. Otol. Neurotol. 22, 340–349. doi:10.1097/00129492-200105000-00012.

Frijns, J.H.M., Briaire, J.J., Schoonhoven, R., 2000. Integrated use of volume conduction and neural models to simulate the response to cochlear implants. Simul. Pract. Theory 8, 75–97.

Frijns, J.H.M., de Snoo, S.L., Schoonhoven, R., 1995. Potential distributions and neural excitation patterns in a rotationally symmetric model of the electrically stimulated cochlea. Hear. Res. 87, 170–186. doi:10.1016/0378-5955(95)00090-Q.

Frijns, J.H.M., Dekker, D.M.T., Briaire, J.J., 2011. Neural excitation patterns induced by phased-array stimulation in the implanted human cochlea. Acta Otolaryngol. 131, 362–370. doi:10.3109/00016489.2010.541939, (Stockh.).

Frijns, J.H.M., Kalkman, R.K., Briaire, J.J., 2009a. Stimulation of the facial nerve by intracochlear electrodes in otosclerosis: a computer modeling study. Otol. Neurotol. 30, 1168–1174. doi:10.1097/MAO.0b013e3181b12115.

Frijns, J.H.M., Kalkman, R.K., Vanpoucke, F.J., Bongers, J.S., Briaire, J.J., 2009b. Simultaneous and non-simultaneous dual electrode stimulation in cochlear implants: evidence for two neural response modalities. Acta Otolaryngol. 129, 433–439. doi:10.1080/00016480802610218, (Stockh.).

Garcia, C., Deeks, J.M., Goehring, T., Borsetto, D., Bance, M., Carlyon, R.P., 2022. SpeedCAP: an efficient method for estimating neural activation patterns using electrically evoked compound action-potentials in cochlear implant users. Ear Hear. Publish Ahead of Print. doi:10.1097/AUD.0000000000001305.

Garcia, C., Goehring, T., Cosentino, S., Turner, R.E., Deeks, J.M., Brochier, T., Rughooputh, T., Bance, M., Carlyon, R.P., 2021. The panoramic ECAP method: estimating patient-specific patterns of current spread and neural health in cochlear implant users. J. Assoc. Res. Otolaryngol. 22, 567–589. doi:10.1007/s10162-021-00795-2.

Gärtner, L., Lenarz, T., Ivanauskaite, J., Büchner, A., 2022. Facial nerve stimulation in cochlear implant users - a matter of stimulus parameters? Cochlear Implants Int. 0, 1–8. doi:10.1080/14670100.2022.2026025.

Herrmann, D.P., Kretzer, K.V.A., Pieper, S.H., Bahmer, A., 2021. Effects of electrical pulse polarity shape on intra cochlear neural responses in humans: triphasic pulses with anodic and cathodic second phase. Hear. Res. 412, 108375. doi:10.1016/j.heares.2021.108375.

Hey, M., Muller-Deile, J., 2015. Accuracy of measurement in electrically evoked compound action potentials. J. Neurosci. Methods 239, 214–222. doi:10.1016/j.jneumeth.2014.10.012.

Hughes, M.L., 2008. A re-evaluation of the relation between physiological channel interaction and electrode pitch ranking in cochlear implants. J. Acoust. Soc. Am. 124, 2711–2714. doi:10.1121/1.2990710.

Joshi, S.N., Dau, T., Epp, B., 2017. A model of electrically stimulated auditory nerve fiber responses with peripheral and central sites of spike generation. J. Assoc. Res. Otolaryngol. 18, 323–342. doi:10.1007/s10162-016-0608-2.

Kalkman, R.K., Briaire, J.J., Dekker, D.M.T., Frijns, J.H.M., 2022. The relation between polarity sensitivity and neural degeneration in a computational model of cochlear implant stimulation. Hear. Res. 415, 108413. doi:10.1016/j.heares.2021.108413.

Kalkman, R.K., Briaire, J.J., Dekker, D.M.T., Frijns, J.H.M., 2014. Place pitch versus electrode location in a realistic computational model of the implanted human cochlea. Hear. Res. 315, 10–24.

Kalkman, R.K., Briaire, J.J., Frijns, J.H.M., 2016. Stimulation strategies and electrode design in computational models of the electrically stimulated cochlea: an overview of existing literature. Netw. Comput. Neural Syst. 27, 107–134. doi:10.3109/0954898X.2016.1171412.

Kalkman, R.K., Briaire, J.J., Frijns, J.H.M., 2015. Current focussing in cochlear implants: an analysis of neural recruitment in a computational model. Hear. Res. 322, 89–98.

Kelsall, D.C., Shallop, J.K., Brammeier, T.G., Prenger, E.C., 1997. Facial nerve stimulation after nucleus 22-channel cochlear implantation. Otol. Neurotol. 18, 336–341.

Kempf, H.G., Tempel, S., Johann, K., Lenarz, T., 1999. Complications of cochlear implant surgery in children and adults. Laryngorhinootologie 78, 529–537. doi:10.1055/s-1999-8753.

Lilly, J.C., Hughes, J.R., Alvord, E.C., Galkin, T.W., 1955. Brief, noninjurious electric waveform for stimulation of the brain. Science 121, 468–469. doi:10.1126/science.121.3144.468.

Macherey, O., Carlyon, R.P., van Wieringen, A., Deeks, J.M., Wouters, J., 2008. Higher sensitivity of human auditory nerve fibers to positive electrical currents. J. Assoc. Res. Otolaryngol. 9, 241–251. doi:10.1007/s10162-008-0112-4.

Medina, G.N.E., Borel, S., Nguyen, Y., Ambert-Dahan, E., Ferrary, E., Sterkers, O., Grayeli, A.B., 2013. Is electrode-modiolus distance a prognostic factor for hearing performances after cochlear implant surgery? Audiol. Neurotol. 18, 406–413.

Miller, C.A., Abbas, P.J., Brown, C.J., 2000. An improved method of reducing stimulus artifact in the electrically evoked whole-nerve potential. Ear Hear. 21, 280–290. doi:10.1097/00003446-200008000-00003.

Miller, C.A., Abbas, P.J., Robinson, B.K., 2001. Response properties of the refractory auditory nerve fiber. J. Assoc. Res. Otolaryngol. 2, 216–232. doi:10.1007/s101620010083.

Miller, C.A., Abbas, P.J., Rubinstein, J.T., Robinson, B.K., Matsuoka, A.J., Woodworth, G., 1998. Electrically evoked compound action potentials of guinea pig and cat: responses to monopolar, monophasic stimulation. Hear. Res. 119, 142–154.

Miller, C.A., Brown, C.J., Abbas, P.J., Chi, S.L., 2008. The clinical application of potentials evoked from the peripheral auditory system. Hear. Res. 242, 184–197. doi:10.1016/j.heares.2008.04.005, Frontiers of auditory prosthesis research: Implications for clinical practice.

Morsnowski, A., Charasse, B., Collet, L., Killian, M., Muller-Deile, J., 2006. Measuring the refractoriness of the electrically stimulated auditory nerve. Audiol. Neurootol. 11, 389–402. doi:10.1159/000095966.

Muckle, R.P., Levine, S.C., 1994. Facial nerve stimulation produced by cochlear implants in patients with cochlear otosclerosis. Am. J. Otol. 15, 394–398.

Nassiri, A.M., Yawn, R.J., Dedmon, M.M., O'Connell, B.P., Holder, J.T., Haynes, D.S., Rivas, A., 2018. Facial nerve stimulation patterns associated with cochlear implantation in labyrinthitis ossificans. Otol. Neurotol. 39, e992–e995. doi:10.1097/MAO.0000000000002028.

Niparko, J.K., Oviatt, D.L., Coker, N.J., Sutton, L., Waltzman, S.B., Cohen, N.L., 1991. Facial nerve stimulation with cochlear implantation. VA cooperative study group on cochlear implantation. Otolaryngol. Head Neck Surg. 104, 826–830. doi:10.1177/019459989110400610.

Pires, J.S., Melo, A.S., Caiado, R., Martins, J.H., Eloi Moura, J., Silva, L.F., 2018. Facial nerve stimulation after cochlear implantation: our experience in 448 adult patients. Cochlear Implants Int. 19, 193–197. doi:10.1080/14670100.2018.1452561.

Polak, M., Ulubil, S.A., Hodges, A.V., Balkany, T.J., 2006. Revision cochlear implantation for facial nerve stimulation in otosclerosis. Arch. Otolaryngol. Head Neck Surg. 132, 398–404. doi:10.1001/archotol.132.4.398.

Potrusil, T., Heshmat, A., Sajedi, S., Wenger, C., Johnson Chacko, L., Glueckert, R., Schrott-Fischer, A., Rattay, F., 2020. Finite element analysis and three-dimensional reconstruction of tonotopically aligned human auditory fiber pathways: a computational environment for modeling electrical stimulation by a cochlear implant based on micro-CT. Hear. Res. 393, 108001. doi:10.1016/j.heares.2020.108001.

Rattay, F., 1999. The basic mechanism for the electrical stimulation of the nervous system. Neuroscience 89, 335–346. doi:10.1016/s0306-4522(98)00330-3.

Rattay, F., Leao, R., Felix, H., 2001a. A model of the electrically excited human cochlear neuron. II. Influence of the three-dimensional cochlear structure on neural excitability. Hear. Res. 153, 64–79. doi:10.1016/S0378-5955(00)00257-4.

Rattay, F., Lutter, P., Felix, H., 2001b. A model of the electrically excited human cochlear neuron: I. Contribution of neural substructures to the generation and propagation of spikes. Hear. Res. 153, 43–63. doi:10.1016/S0378-5955(00)00256-2.

Rayner, M.G., King, T., Djalilian, H.R., Smith, S., Levine, S.C., 2003. Resolution of facial stimulation in otosclerotic cochlear implants. Otolaryngol. Head Neck Surg. 129, 475–480. doi:10.1016/s0194-5998(03)01444-x.

Resnick, J.M., O'Brien, G.E., Rubinstein, J.T., 2018. Simulated auditory nerve axon demyelination alters sensitivity and response timing to extracellular stimulation. Hear. Res. 361, 121–137. doi:10.1016/j.heares.2018.01.014.

Rotteveel, L.J., Proops, D.W., Ramsden, R.T., Saeed, S.R., van Olphen, A.F., Mylanus, E.A., 2004. Cochlear implantation in 53 patients with otosclerosis: demographics, computed tomographic scanning, surgery, and complications. Otol. Neurotol. 25, 943–952. doi:10.1097/00129492-200411000-00014.

Rowland, V., Macintyre, W.J., Bidder, T.G., 1960. The production of brain lesions with electric currents. II. Bidirectional currents. J. Neurosurg. 17, 55–69. doi:10.3171/jns.1960.17.1.0055.

Schart-Moren, N., Larsson, S., Rask-Andersen, H., Li, H., 2017. Anatomical characteristics of facial nerve and cochlea interaction. Audiol. Neurootol. 22, 41–49. doi:10.1159/000475876.

Seyyedi, M., Herrmann, B.S., Eddington, D.K., Nadol, J.B.J., 2013. The pathologic basis of facial nerve stimulation in otosclerosis and multi-channel cochlear implantation. Otol. Neurotol. 34, 1603–1609. doi:10.1097/MAO.0b013e3182979398.

Shannon, R.V., Zeng, F.G., Kamath, V., Wygonski, J., Ekelid, M., 1995. Speech recognition with primarily temporal cues. Science 270, 303–304. doi:10.1126/science.270.5234.303.

Snel-Bongers, J., Briaire, J.J., van der Veen, E.H., Kalkman, R.K., Frijns, J.H.M., 2013. Threshold levels of dual electrode stimulation in cochlear implants. J. Assoc. Res. Otolaryngol. 14, 781–790. doi:10.1007/s10162-013-0395-y.

Spoendlin, H., 1972. Innervation densities of the cochlea. Acta Otolaryngol. 73, 235–248. doi:10.3109/00016487209138937, (Stockh.).

Undurraga, J.A., van Wieringen, A., Carlyon, R.P., Macherey, O., Wouters, J., 2010. Polarity effects on neural responses of the electrically stimulated auditory nerve at different cochlear sites. Hear. Res. 269, 146–161. doi:10.1016/j.heares.2010.06.017.

Wobbrock, J.O., Findlater, L., Gergle, D., Higgins, J.J., 2011. The aligned rank transform for nonparametric factorial analyses using only anova procedures. In: Proceedings of the SIGCHI Conference on Human Factors in Computing Systems, CHI '11, New York, NY, USA. Association for Computing Machinery, pp. 143–146. doi:10.1145/1978942.1978963.